Advanced Steel Construction – Vol. 19 No. 1 (2023) 31–37
DOI:10.18057/IJASC.2023.19.1.5
(**Special Issue:** *10th International Conference on Advances in Steel Structures, ICASS'2020, Chengdu, China*)

ELASTIC BUCKLING OF OUTSTAND STAINLESS-CLAD BIMETALLIC STEEL PLATES

Yi-Xiao Mei and Hui-Yong Ban *

Department of Civil Engineering, Tsinghua University, Beijing, PR China
** (Corresponding author: E-mail: banhy@tsinghua.edu.cn)*

ABSTRACT

The application of stainless-clad (SC) bimetallic steel in various conditions such as offshore and marine environment requires members designed in different cross-sectional shapes, which consist of both internal and outstand elements. To form a comprehensive understanding of buckling behaviour of the SC bimetallic steel members, the behaviour of outstand compression plates needs to be investigated. In this study, the theoretical elastic buckling stress of outstand SC bimetallic steel plates subjected to uniformly distributed uniaxial compression is derived. Considering the position of neutral surface, the energy method and Ritz formulation are used to solve the buckling stress. Adaptation of the first-order shear deformation plate theory (FSDT) is used to modify the solution, which is further compared with finite element analyses. The influence of different parameters such as cladding configuration, clad ratio, elastic modulus ratio, aspect ratio and width-to-thickness ratio on the elastic buckling behaviour of the SC bimetallic plates is analysed. The simplified design formulae and design requirements are summarized to form a comprehensive design method.

ARTICLE HISTORY

Received: 20 July 2022
Revised: 22 August 2022
Accepted: 10 January 2023

KEYWORDS

Stainless-clad bimetallic steel plate;
Elastic buckling;
Uniaxial compression;
First-order shear deformation plate theory (FSDT);
Outstand plates

1. Introduction

As an advanced high-performance laminated steel, stainless-clad (SC) bimetallic steel has been increasingly utilised in engineering structures in recent years. The SC bimetallic steel consists of two types of metallurgically bonded layers, i.e., the cladding layer made of stainless steel and the substrate layer made of conventional mild (CM) steel, which can provide remarkable corrosion resistance and economic efficiency, respectively. By virtue of these overwhelming advantages, the SC bimetallic steel has already been successfully applied in high-rise buildings and steel bridges and is considered as a new solution for infrastructures against environmental corrosion, such as offshore and marine structures.

The research advances of SC bimetallic steel structures have been previously reviewed by the authors [1]. A series of comprehensive studies on full-life cycle material properties of SC bimetallic steel hitherto have been reported, in which different service conditions including fire [2], post-fire loading [3], marine atmospheric corrosion [4], cyclic loading [5] and impact loading [6] are considered. On the topic of mechanical performance of structural members, limited but increasing attention has been paid to SC bimetallic steel members such as plates [7], columns [8] and connections [9].

Compression is one of the major types of loads applied to steel structures, and for steel structure members under compression, buckling is one of the most essential failure modes of engineering design. For a novel structural material such as SC bimetallic steel, there is very limited research addressing the buckling mechanism. Therefore, a series of basic studies looking into the stability of SC bimetallic steel members, from plates to columns, have been conducted by the authors. Combining theoretical analyses ranging from elastic to inelastic stages [7] as well as experimental investigations of stub and long columns [8], the authors aim at establishing a set of buckling design methods which can provide a solid foundation for the future application of SC bimetallic steel in structures.

A previous paper presented by the authors [7] addresses the elastic buckling of internal SC bimetallic steel plates in hollow section columns or I-section columns, which can be also refereed to simply supported plates. The nominal elastic buckling stress of such plates is derived using two different theories, i.e., the classical plate theory (CPT) and the first-order shear deformation plate theory (FSDT). Validated by finite element models, the FSDT solutions are adopted to carry on parametric studies on the effects of key factors such as cladding configuration, clad ratio, elastic modulus ratio and width-to-thickness ratio on the elastic buckling stress. Furthermore, a simplified design method to calculate elastic buckling stress in an efficient and accurate way has been proposed, along with the design requirements for bonding interface shear strength.

Since the previous studies on SC bimetallic steel structures mainly focus on the hollow section members and simply supported plates in these sections, there is a lack of attention paid to the outstand (three edges simply supported and one edge free of support) plates shown in Fig. 1(a). Although the hollow sections such as square hollow sections (SHS), rectangular hollow sections (RHS) and circular hollow sections (CHS) are the most suitable sections for SC bimetallic steel because it can allow the cladding layer whose corrosion resistance is excellent to be put on the outside, while the substrate layer made of CM steel to be protected inside. However, in practice many structures have to be designed with columns or beams using open sections such as I-sections or C-sections. In such sections, there are not only simply supported boundary conditions, but also plates with three edges simply supported and one edge free of support. Therefore, the need for studying the elastic buckling of outstand plates is of the same importance as that for internal plates.

In the present work, on the basis of the previous study, the elastic buckling behaviour of outstand plates subjected to uniaxial compression is thoroughly investigated. The comparison of internal and outstand plates in a common I-section column is illustrated in Fig. 1(a). With consideration of the position of neutral surface as well as the first-order shear deformation plate theory, the energy method is utilised to derive the closed-form analytical solution of the buckling stress, which is further compared with finite element analyses results. Effects of cladding configuration, clad ratio, elastic modulus ratio, aspect ratio and width-to-thickness ratio on the elastic buckling behaviour are investigated by parametric study. A set of simplified formulae for the calculation of buckling stress is proposed in order to establish a complete design method.

2. Theoretical derivation

2.1. Basic assumptions

The theoretical analysis is based on the following assumptions for simplification and generalization: (1) The materials are homogeneous and linear elastic; (2) The plate is ideally flat without geometric imperfections or residual stresses; (3) Membrane stresses due to the small deflection can be neglected; (4) The load is uniformly distributed on the edge of the plate.

For the reason that the outstand plates may be adopted in structural members with different cross-sections, two cladding configurations are considered in this study: plates with singly-sided cladding metal (denoted by SP) and plates with doubly-sided cladding metal (denoted by DP), as illustrated in Fig. 1(b). The boundary conditions and buckling mode are also included in Fig. 1(b). The clad ratio β is defined as a ratio of the thickness of the cladding layer(s) to the overall thickness of the plate t. Accordingly, the thickness of the cladding layer in SP is βt; the DP are simplified to be symmetrically laminated herein, thus the two cladding layers are both $0.5\beta t$ thick.

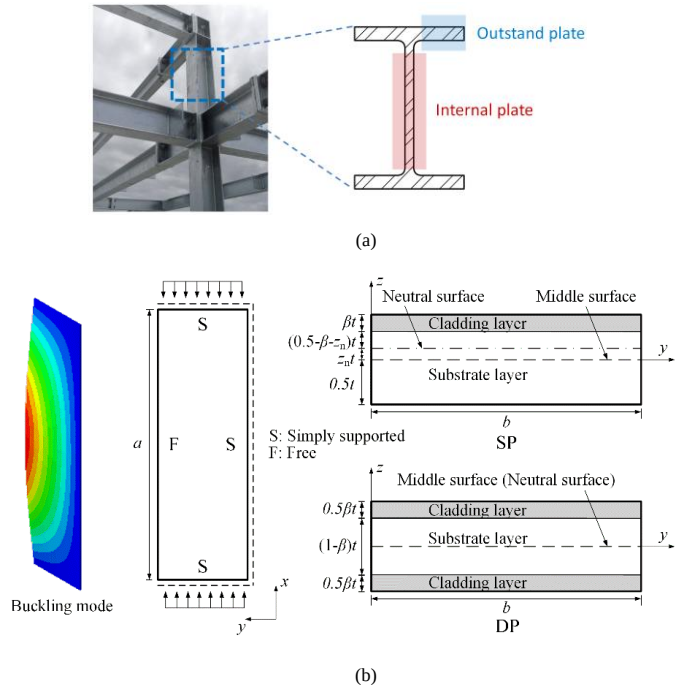

Fig. 1 Illustration of (a) internal and outstand plates in an I-section column; (b) boundary conditions and cladding configurations of outstand plates.

As discussed in many studies [10,11], the middle surface may not coincide with the physical neutral surface due to the unsymmetrical configuration of plate. To eliminate the coupling phenomenon between transverse bending and in-plane stretching during deformation as well as to avoid additional moment caused by eccentricity, the uniformly distributed load is considered to be applied within the neutral surface. In the case of SP, the relative position of neutral surface from the middle one can be calculated by [7]:

$$z_{\mathrm{n}} = \frac{\beta(1-\beta)(E_{\mathrm{c}}-E_{\mathrm{s}})}{2[\beta E_{\mathrm{c}}+(1-\beta)E_{\mathrm{s}}]}, \tag{1}$$

in which E_{s} and E_{c} are the elastic moduli of substrate and cladding materials, respectively.

Eq. (1) shows that the relative position of neutral surface from the middle one z_{n} depends on clad ratio as well as the elastic moduli of the two component metals. When the elastic modulus of the substrate material is larger than that of the cladding material, which is the case of SC bimetallic steel or other common bimetallic steel such as titanium-clad (TC) bimetallic steel, z_{n} is always no larger than zero. As the clad ratio increases, the absolute value of z_{n} grows until a certain value of clad ratio is reached, this value is usually around 0.5 and depends on the ratio of elastic moduli $E_{\mathrm{c}}/E_{\mathrm{s}}$. For SC bimetallic steel, the highest absolute value of z_{n} is 0.008, which is relatively moderate, while for TC bimetallic steel, this value can rise to 0.086, which is quite considerable for plate analysis. In order to ensure the accuracy and maintain consistency with the previous work, z_{n} will be taken into consideration in the following analysis.

2.2. Ritz formulation and solution for the buckling stress

The buckling stress of a homogeneous outstand plate can be solved by the energy method with Ritz formulation [12]. Based on the boundary conditions of outstand plate and coordinate system shown in Fig. 1(b), the deflection ω can be expressed by the Ritz approximation of rectangular plates:

$$\omega = fy\sin\frac{m\pi x}{a} \tag{2}$$

The strain energy Π_{i} and external potential energy Π_{e} can be written as:

$$\Pi_{\mathrm{i}} = \frac{D}{2}\int_0^a\int_0^b\left\{\left(\frac{\partial^2\omega}{\partial x^2}+\frac{\partial^2\omega}{\partial y^2}\right)^2 - 2(1-\nu)\left[\frac{\partial^2\omega}{\partial x^2}\times\frac{\partial^2\omega}{\partial y^2}-\left(\frac{\partial^2\omega}{\partial x\partial y}\right)^2\right]\right\}\mathrm{d}x\mathrm{d}y \tag{3}$$

$$\Pi_{\mathrm{e}} = -\frac{1}{2}\int_0^a\int_0^b\sigma_x t\left(\frac{\partial\omega}{\partial x}\right)^2\mathrm{d}x\mathrm{d}y \tag{4}$$

where D is the bending stiffness of the plate, which will be discussed later.

The principle of minimum total potential energy requires that the first variation of total potential energy equals to zero:

$$\delta\Pi = \delta(\Pi_{\mathrm{i}}+\Pi_{\mathrm{e}}) = 0 \tag{5}$$

Because $f\neq 0$ when buckling occurs, by substituting Eqs. (2)-(4) into Eq. (5) and setting constant m=1 and ν=0.3, the buckling stress σ_{cr} can be expressed as:

$$\sigma_{\mathrm{cr}} = \left(0.425+\frac{b^2}{a^2}\right)\frac{\pi^2 D}{b^2 t} \tag{6}$$

The bending stiffness D is denoted as D_{sp} for SP and D_{dp} for DP, which is identical between internal and outstand SC bimetallic steel plate and has been derived in the previous study [7] as follows:

$$D_{\mathrm{sp}} = \int_{-t/2}^{t/2} Q_{11}(z-z_{\mathrm{n}}t)^2\,dz = \frac{t^3}{12(1-\nu^2)}E_{\mathrm{sp}} \tag{7}$$

$$E_{\mathrm{sp}} = [E_{\mathrm{c}}(4\beta^3-6\beta^2+3\beta)+E_{\mathrm{s}}(-4\beta^3+6\beta^2-3\beta+1)]+12z_{\mathrm{n}}\beta(\beta-1)(E_{\mathrm{c}}-E_{\mathrm{s}})+12z_{\mathrm{n}}^2[\beta E_{\mathrm{c}}+(1-\beta)E_{\mathrm{s}}] \tag{8}$$

$$D_{\mathrm{dp}} = \int_{-t/2}^{t/2} Q_{11}z^2\,dz = \frac{t^3}{12(1-\nu^2)}E_{\mathrm{dp}} \tag{9}$$

$$E_{\mathrm{dp}} = E_{\mathrm{c}}(\beta^3-3\beta^2+3\beta)+E_{\mathrm{s}}(-\beta^3+3\beta^2-3\beta+1) \tag{10}$$

The main difference between the expression of E_{sp} and E_{dp} is that the former one involves z_{n} so it is more complicated. On the contrary, because the laminar structure of DP is symmetric (i.e. $z_{\mathrm{n}}=0$), the expression of is E_{dp} simple.

2.3. Influence of transverse shear deformation

Due to the difficulty of establishing and solving the FSDT-based governing equations of outstand SC bimetallic steel plates, a simplified method has been adopted herein to consider the influence of transverse shear deformation independently. The buckling stress is modified by introducing the shear deformation effect factor k_{FSDT} [7]:

$$\sigma_{\mathrm{cr,FSDT}} = k_{\mathrm{FSDT}}\times\left(0.425+\frac{b^2}{a^2}\right)\frac{\pi^2 D}{b^2 t} \tag{11}$$

$$k_{\mathrm{FSDT}} = 1-\frac{2\chi}{2\chi+1-\nu} \tag{12}$$

$$\chi = \frac{\pi^2}{12K_{\mathrm{s}}}\left(\frac{t}{b}\right)^2\left(\frac{1}{(a/b)^2}+1\right) \tag{13}$$

where K_{s} is the shear correction factor.

The derivation of the shear deformation effect factor k_{FSDT} and the shear correction factor K_{s} can be found in literature [7]. In this study, in order to keep the concision and to avoid repetition, the whole expression of K_{s} is not presented herein due to its extraordinarily complicated form. The mathematical software MATLAB is employed to calculate K_{s} in the validation and parametric analyses while specific values are listed in tables for engineering design.

3. Validation and parametric analyses

3.1. Validation against numerical results

The theoretical solution of the buckling stress $\sigma_{\mathrm{cr,FSDT}}$ expressed by Eq. (11) is validated in two ways through FE analyses, i.e., MATLAB and ABAQUS. The MATLAB codes developed by Ferreira [13] have been modified by the authors to include the boundary condition of outstand plates. The bending stiffness and transverse shear stiffness have also been modified to the equivalent ones of bimetallic steel plates. The FE models of bimetallic steel plates are developed in ABAQUS for eigenvalue buckling analysis. The shell offset calculated by Eq. (1) has been incorporated in the models so that the uniformly distributed load is applied exactly within the neutral surface. Since the first order buckling mode for outstand plates subjected to uniaxial compression is known to be symmetric, only half of the plate is modelled to save the computing time. With proper consideration for the influence of transverse shear deformations, the codes used in MATLAB and the models developed in ABAQUS can both calculate the buckling stress of bimetallic steel outstand plates under the assumption of FSDT.

To ensure the consistency of the two methods, the four-node quadrilateral

element Q4 defined by Ferreira [13] is used in MATLAB while the four-node quadrilateral shell element with reduced integration S4R is used in ABAQUS. In both ways of FE analyses, the number of elements on the loaded edges is set as twenty while the number of elements on the other two edges changes with the aspect ratio a/b to make sure the elements are square. The elastic moduli of the cladding and substrate materials are taken as E_c=1.93×10^{5}MPa and E_s=2.06×10^{5}MPa, respectively, according to the Chinese standards [14,15].

Two cladding configurations illustrated in Fig. 1(b) are considered while different clad ratios, width-to-thickness ratios, aspect ratios and cladding materials are used for the purpose of validation. The theoretical solutions $\sigma_{cr,FSDT}$ are compared with the FE analysis results $\sigma_{cr,MATLAB}$ and $\sigma_{cr,ABAQUS}$ in Table 1 through 12 groups of data. In each group, 11 clad ratios between 0 and 1 are considered, while one typical group of results is plotted in Fig. 2. In Table 1, the cladding type consists of two parts; the first part represents the cladding configuration (i.e. SP and DP) while the second part represents the cladding material. SC is the stainless-clad bimetallic steel defined above while TC is the titanium-clad bimetallic steel, whose cladding material is replaced by titanium with an elastic modulus of 1.03×10^{5}MPa.

The comparison of FE analysis results $\sigma_{cr,MATLAB}$ and $\sigma_{cr,ABAQUS}$ suggests that the FE analysis methods have complete consistency with each other, which can verify the adequacy of the FE models. It can be seen from Table 1 and Fig. 2 that, the theoretical solutions derived herein agree well with both MATLAB and ABAQUS analysis results, which means the proposed theory herein is particularly accurate for elastic buckling analysis of outstand SC bimetallic steel plates in a wide range of parameters.

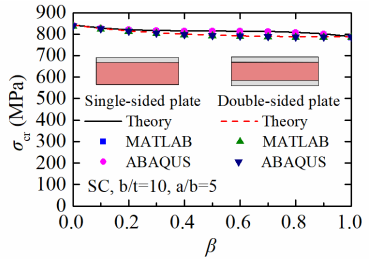

Fig. 2 Comparison of two typical groups of results (SP and DP, SC, b/t=10, a/b=5)

Table 1
Comparison between theoretical solutions with FE analysis results

Group	Cladding Type	b/t	a/b	$\sigma_{cr,ABAQUS}/\sigma_{cr,FSDT}$		$\sigma_{cr,ABAQUS}/\sigma_{cr,MATLAB}$	
				Mean	COV	Mean	COV
1	SP, SC	10	5	0.998	0.000	1.003	0.000
2	SP, SC	15	5	0.993	0.000	1.001	0.000
3	SP, SC	20	5	0.993	0.000	1.001	0.000
4	SP, SC	50	5	0.996	0.000	1.001	0.000
5	SP, SC	20	3	0.990	0.000	1.001	0.000
6	SP, SC	20	1	0.987	0.000	1.003	0.000
7	SP, TC	10	5	0.999	0.001	1.003	0.000
8	SP, TC	20	5	0.993	0.001	1.001	0.000
9	DP, SC	10	5	0.998	0.000	1.003	0.000
10	DP, SC	20	5	0.993	0.000	1.001	0.000
11	DP, TC	10	5	1.000	0.001	1.003	0.000
12	DP, TC	20	5	0.994	0.001	1.001	0.000

3.2. Parametric analyses

Based on the validated theoretical solutions, a series of parametric analyses have been carried out, in which the effects of clad ratio, width-to-thickness ratio, aspect ratio, cladding configuration and cladding material are clarified. The buckling stress $\sigma_{cr,FSDT}$ is calculated according to Eqs. (11)-(13), in which K_s is computed with the help of MATLAB.

3.2.1. Influence of clad ratio

The influence of clad ratio on the buckling stress $\sigma_{cr,FSDT}$ is already shown in Fig. 2 that with an increase of clad ratio, the buckling stress decreases. Although the start and end points are the same, the downward trends of SP and DP are distinctly different. There is a plateau in the middle section of the SP curve and steep slopes in the edge sections, while the slope of the DP curve is gradually descending as the clad ratio increases. While the overall downward trend can be explained by the smaller elastic modulus of the cladding material compared to that of the substrate one, the cause of difference between SP and DP curves should be further clarified.

It can be known from Eqs. (11)-(13) that for plates with identical dimensions, the buckling stress is influenced by the bending stiffness D and the shear deformation effect factor k_{FSDT}. The variation of both parameters with the clad ratio is shown in Fig. 3. It can be found that the shapes of bending stiffness curves are quite similar to those of buckling stress curves , while the shear deformation effect factor curves have different shapes from the buckling stress curves and their variation is slight. Hence, it can be concluded that the influence of clad ratio is predominately reflected in the bending stiffness.

The difference between the bending stiffness D between SP and DP can be explained by Eqs. (7) and (9). Since the bending stiffness is calculated by integration, for one specific point within the plate, the further it is from the neutral axis through the thickness direction, the greater its influence on the integral result will be. For the unsymmetric structure possessed by SP, when the clad ratio is very small or very large, the variation of clad ratio can be regarded as substituting the material near the external surface. For such position, since its distance from the neutral surface is large, the influence on the integration result of bending stiffness is significant. On the other hand, when the clad ratio is around 0.5, the change of clad ratio means replacing the material in the middle, which can hardly change the bending stiffness since z_n is very small. Whilst for the symmetric DP, since the cladding layers are placed on the outside, as the clad ratio increases, the material is changed from substrate material into cladding material, and this change takes place from outside to inside, resulting in the gradually descending slope of bending stiffness curve.

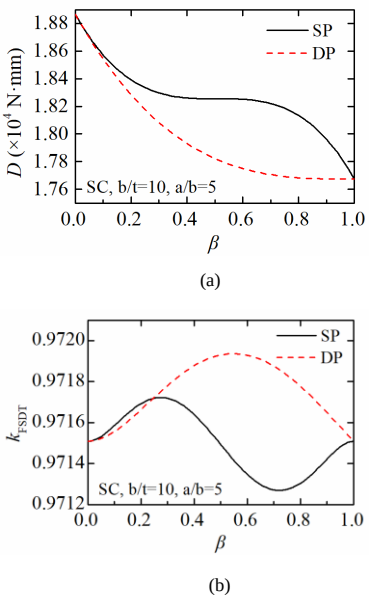

Fig. 3 Influence of clad ratio on (a) bending stiffness; (b) shear deformation effect factor

3.2.2. Influence of width-to-thickness ratio

Fig. 4 shows the influence of width-to-thickness ratio b/t on the buckling stress, in which different cladding configurations, clad ratios and cladding materials are also taken into consideration. The range of b/t is between 10 and 80 to cover both moderately thick plates and thin plates. It can be concluded from the Fig. 4 that when the width-to-thickness ratio is below 30, the buckling stress decreases with b/t rapidly; the descending rate slows as b/t becomes larger. This trend is in accordance with the expression of plate buckling stress Eq. (11).

It can also be seen that for SC bimetallic steel plates, the variation of clad ratio has very limited influence on the buckling stress comparing to the variation of width-to-thickness ratio. In comparison, the difference between curves of different clad ratio is clear when the cladding material is changed from stainless steel into titanium, as illustrated in Figs. 4(c) and 4(d). This phenomenon can be explained by the elastic modulus. Since the substrate material is fixed, when the cladding material is stainless steel whose elastic modulus is similar to that of CM steel, the difference between the two metals is slight and the influence of clad ratio is thus insignificant. However, when the cladding material is titanium, its elastic modulus is only half of that of CM steel, which leads logically to a more considerable effect.

It should be noticed that in Fig. 4(d), when the clad ratio is small (from 0.1 to 0.5), the difference between curves is visible, but as the clad ratio continues

to grow, the curves of β=0.5, 0.7 and 0.9 have rather limited distinction. This can be clarified by the DP curve shown in Fig. 3(a), when clad ratio is small the variation of clad ratio has a strong impact on the buckling stress, whilst the impact is considerably diminished when the clad ratio becomes larger.

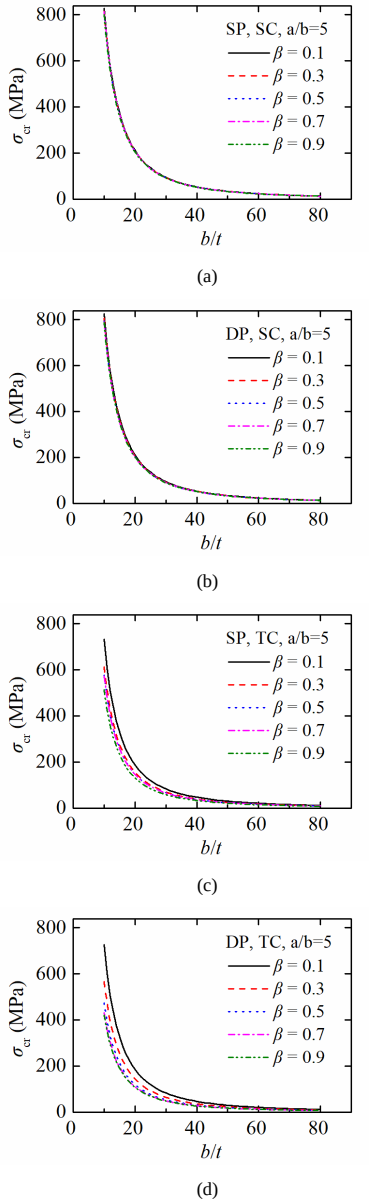

Fig. 4 Influence of width-to-thickness ratio on the buckling stress of (a) SP, SC; (b) DP, SC; (c) SP, TC; (d) DP, TC.

3.2.3. Influence of aspect ratio

A similar trend can be observed in Fig. 5 with respect of the influence of the aspect ratio *a*/*b*. Several factors such as cladding configurations, clad ratios and cladding materials are considered as well. From 1 to 10, the range of aspect ratio *a*/*b* covers both square plate and long rectangular plate. When the aspect ratio is below 4, the buckling stress decreases with *a*/*b* rapidly; the descending rate goes down as *a*/*b* grows. The expression of plate buckling stress Eq. (11) can once again be used to explain this trend, as the reciprocal of the aspect ratio has been squared and placed in bracket. Similar to what we have found in the study of width-to-thickness ratio, the variation of clad ratio has very limited influence on the buckling stress compared with the variation of aspect ratio for SC bimetallic steel plates, and the gap between curves of different clad ratios is wider when stainless steel is replaced by titanium as the cladding material. This phenomenon can be also explained by the elastic modulus the same way as it has been clarified in last section.

Fig. 5(c) shows that the difference between curves changes with the clad ratio, when the clad ratio is rather small or large, the gap between curves is visible. For clad ratios between 0.3 and 0.7, the curves are very close to each other. In Fig. 5(d), it has been also found that when the clad ratio is small (0.1~0.3), the difference between curves is visible, while the curves of larger clad ratio show minor difference. The SP and DP curves shown in Fig. 3(a) can offer a reasonable explanation, as the influence of clad ratio on the buckling stress varies for different clad ratios and cladding configurations.

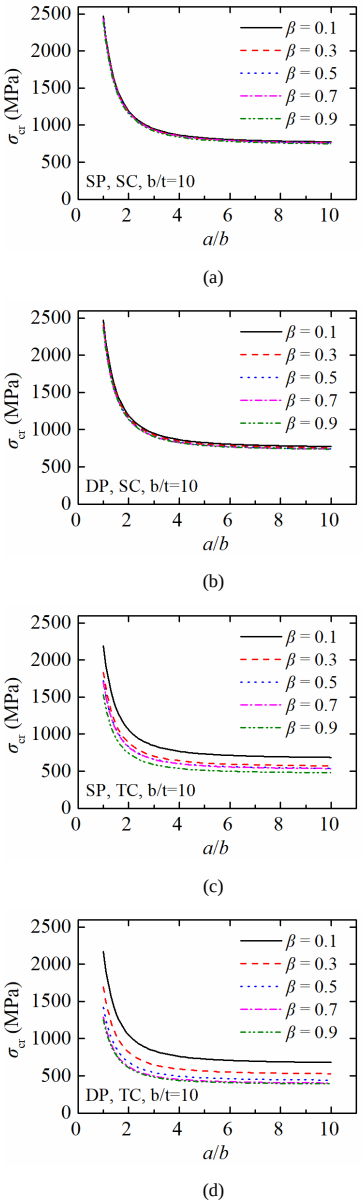

Fig. 5 Influence of aspect ratio on the buckling stress of (a) SP, SC; (b) DP, SC; (c) SP, TC; (d) DP, TC.

3.2.4. Influence of cladding metal

If the cladding metal is replaced by others, the elastic modulus E_c will become different and thus the elastic buckling stress will be influenced. In Fig. 6, the elastic modulus ratio E_c /E_s is selected as the abscissa to demonstrate the influence of cladding metal. It can be seen that as the elastic modulus of the cladding metal increases, the buckling strength grows in a quasi-linear way. For SP with clad ratios around 0.5, when the elastic modulus of the cladding metal reduces to a substantial degree, i.e. below 60% of that of the substrate metal, the buckling strength of plates drops a little bit more quickly. The influence of clad ratio on the buckling stress decreased as the elastic modulus ratio gradually approaches 1 due to the similarity of cladding and substrate materials. Three different combinations of with-to-thickness ratio and aspect ratio as well as five different clad ratios has been used to conduct a more comprehensive analysis of the influence of cladding material. Through Figs. 6(a)~6(e), it can be found that the shapes of curves in different figures are very similar albeit the width-to-thickness ratio and aspect ratio are different.

Generally, for SP, the curves of β=0.3, 0.5 and 0.7 are similar to each other, while the curves of β=0.1 and 0.9 show considerable difference. For DP, the curves of β=0.5, 0.7 and 0.9 are similar to each other, while the curves of β=0.1 and 0.3 show considerable difference. As analysed in the previous section, this phenomenon can be explained by the influence of clad ratio on the buckling stress shown in Fig. 2 and Fig. 3(a).

In engineering application, the clad ratio used for bimetallic steel is small in most cases due to the consideration of cost and efficiency. For example, the

SC bimetallic steel built-up square hollow section stub columns studied in literature [8] were designed to have clad ratios of 0.207 and 0.391. Hence, more attention should be addressed to the range of small clad ratios. Within the clad ratio ranging from 0.1 to 0.5, the influence of cladding metal suggests that for SC bimetallic steel plates whose elastic modulus ratio E_c/E_s is around 0.94, the effect of parameters is subtle and thus the design method of stainless steel plates can be adopted with necessary slignt modification. . For TC bimetallic steel, a small change of important parameters will lead to a substantial difference in buckling stress, so more attention should be paid when considering the influence of different factors such as clad ratio and width-to-thickness ratio.

To summarize, the cladding metal is critical to the buckling stress of bimetallic steel plates. When the material properties of the cladding and substrate materials such as elastic moduli have significant difference, the slight change of other parameters such as clad ratio and width-to-thickness ratio will cause a big change to the buckling stress.

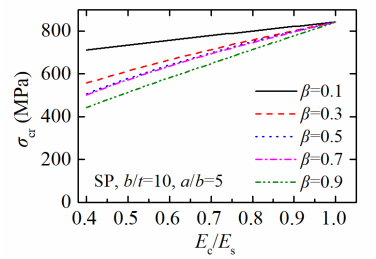

(a)

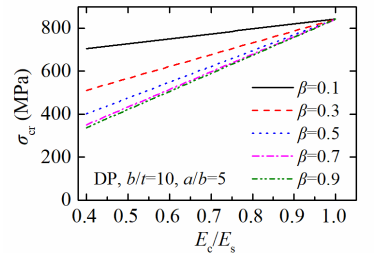

(b)

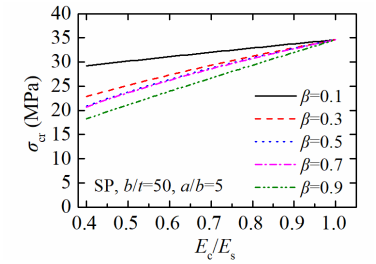

(c)

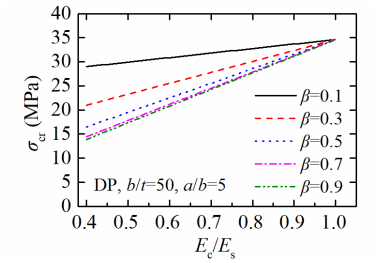

(d)

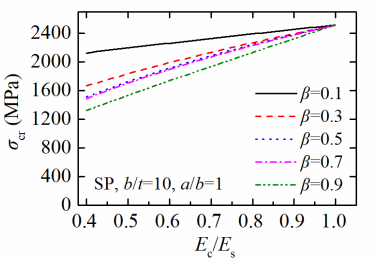

(e)

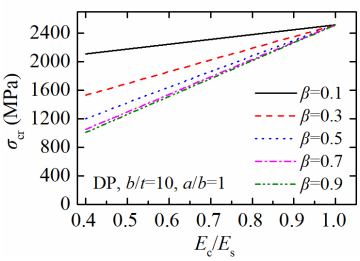

(f)

Fig. 6 Influence of cladding metal on the buckling stress of (a) SP, b/t=10, a/b=5; (b) DP, b/t=10, a/b=5; (c) SP, b/t=50, a/b=5; (d) DP, b/t=50, a/b=5; (e) SP, b/t=10, a/b=1; (f) DP, b/t=10, a/b=1.

3.2.5. Influence of boundary condition

Since the elastic buckling of simply supported (internal) bimetallic steel plates has been investigated in a previous study [7], it is worthwhile to compare the buckling stresses of outstand plates with those of internal plates to find out the influence of boundary condition, and thus to gain a deeper knowledge of the elastic buckling of bimetallic steel plates.

The data of simply supported bimetallic steel plates given in [7] are compared with those of outstand plates herein. The parameters of plates are determined in accordance to the previous study, as the three clad ratios 0.2, 0.5 and 0.8 and two cladding configurations SP and DP are considered. Figs. 7(a) and 7(b) show the results with various elastic modulus ratios E_c/E_s while the width-to-thickness ratio is set as 10 and the shape of the plates is square. Figs. 7(c) and 7(d) demonstrate the results with different width-to-thickness ratios while the material is TC bimetallic steel and the shape of the plates is also square.

It can be seen from Fig. 7 that due to the different boundary conditions, the elastic buckling stress of outstand plates is significantly smaller than that of the internal plates. It needs to be noted that the curves of internal and outstand plates in Fig. 7 have similar shape, which means the variation of buckling stress with both elastic modulus ratio E_c/E_s and width-to-thickness ratio is not profoundly influenced by the change of boundary conditions.

In recognition of the similarity of internal and outstand plates with regard to the variation of buckling stress, the design method of outstand plates can be established on this basis. For the simplicity and convenience of engineering application, a similar way can be applied with only a few key parameters to be updated.

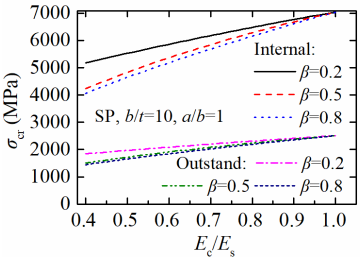

(a)

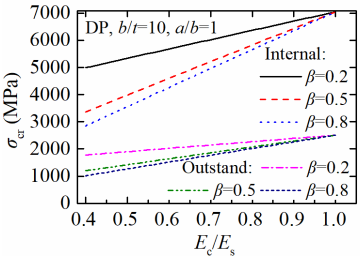

(b)

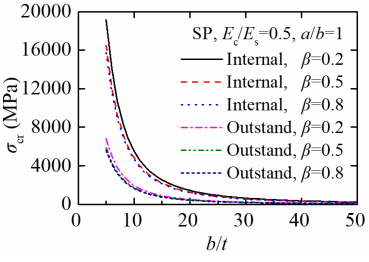

(c)

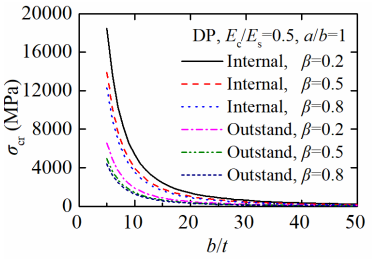

(d)

Fig. 7 Influence of boundary condition on the buckling stress of (a) SP, b/t=10, a/b=1; (b) DP, b/t=10, a/b=1; (c) SP, E_c/E_s=0.5, a/b=1; (d) DP, E_c/E_s=0.5, a/b=1;

4. Design methods

Since the theoretical derivation has been validated against numerical analyses and the influence of critical parameters has been clarified, the design methods for the elastic buckling of outstand SC bimetallic steel plates can be provided. In the authors' previous study on the internal (simply supported) plates, the simplified solution of critical buckling stress has been proposed along with the design requirements for interface shear strength. However, for outstand plates, the transverse shear stresses can't be explicitly expressed by any formula because the buckling stress is solved by the energy method with Ritz formulation.

Therefore, the design methods proposed herein will focus on the calculation of critical buckling stress of bimetallic steel plates. Given that the design methods to calculate the buckling stress of simply supported plates have already been provided in literature [7], they can be combined with the research findings hereinto form a set of integrated and generall design formulae for both oustand and interal elastic buckling of bimetallic steel plates.

By substituting the shear deformation effect factor k_{FSDT} (expressed as Eq. (12)) into the expression of the buckling stress $\sigma_{\mathrm{cr,FSDT}}$ (expressed as Eq. (11)), the buckling stress of internal and outstand plates can be expressed by a unified equation as shown in Eq. (14):

$$\sigma_{\mathrm{cr}}=\frac{\left(1-\frac{2\chi_{\mathrm{int(out)}}}{2\chi_{\mathrm{int(out)}}+1-\nu}\right)k_{\mathrm{int(out)}}\pi^2 D}{b^2 t} \tag{14}$$

In Eq. (14), the parameters $k_{\mathrm{int(out)}}$ and $\chi_{\mathrm{int(out)}}$ varies with the boundary conditions.

For internal plates:

$$k_{\mathrm{int}}=\left(\frac{mb}{a}+\frac{n^2 a}{mb}\right)^2 \tag{15}$$

$$\chi_{\mathrm{int}}=\frac{t^2\pi^2}{12K_{\mathrm{s}}}\left(\frac{m^2}{a^2}+\frac{n^2}{b^2}\right) \tag{16}$$

in which the coefficients m and n are positive integers that results in a lowest k_{int}, which is determined by the aspect ratio of the plates.

For outstand plates:

$$k_{\mathrm{out}}=\left(0.425+\frac{b^2}{a^2}\right) \tag{17}$$

$$\chi_{\mathrm{out}}=\frac{\pi^2}{12K_{\mathrm{s}}}\left(\frac{t}{b}\right)^2\left(\frac{1}{(a/b)^2}+1\right) \tag{18}$$

The shear correction factor K_{s} and bending stiffness D are different for two cladding configurations. The expressions of bending stiffness have been given in Eqs. (7)~(10), and the expressions of are K_{s} as follows:

For plates with singly-sided cladding metal (SP):

$$K_s=\frac{t^5 E_{\mathrm{sp}}^2}{144E_{\mathrm{eq}}h_{\mathrm{s}}(z)} \tag{19}$$

in which E_{sp} is the integral elastic modulus of SP, as shown in Eq. (8); $h_{\mathrm{d}}(z)$ is a complicated parameter whose expanded form is too long to be introduced here. The expanded form can be found in the Appendix A of literature [7]. Another parameter appears in Eq. (19) is the equivalent elastic modulus of the plate E_{eq}, which is same for both SP and DP plates:

$$E_{\mathrm{eq}}=\beta E_{\mathrm{c}}+(1-\beta)E_{\mathrm{s}} \tag{20}$$

For plates with doubly-sided cladding metal (DP):

$$K_s=\frac{t^5 E_{\mathrm{dp}}^2}{144E_{\mathrm{eq}}h_{\mathrm{d}}(z)} \tag{21}$$

in which E_{dp} is the integral elastic modulus of DP, as shown in Eq. (10); E_{eq} is the equivalent elastic modulus of the plate as expressed in Eq. (20); $h_{\mathrm{d}}(z)$ is a complicated parameter whose expanded form can be also found in the Appendix A of literature [7].

Although it is hard to establish a simplified expression or a fitting function for the shear correction factor K_{s}, the authors have suggested a solution for engineering application, that is to use tables for engineers to look up from, as shown in Table 2 for common paraters in practice, while more tables corresponding to different elastic modulus ratios and clad ratios can be provided in the design code to cover the whole range of engineering application. With the help of such tables, one can conveniently find the approximate shear correction factor value of a specific bimetallic steel plate using the tables and linear interpolation.

Table 2
The shear correction factor K_{s} for different bimetallic steel types and cladding configurations

Clad ratio	Shear correction factor K_s			
	SC bimetallic steel		TC bimetallic steel	
	SP	DP	SP	DP
0	0.8333	0.8333	0.8333	0.8333
0.05	0.8340	0.8337	0.8367	0.8351
0.10	0.8355	0.8347	0.8456	0.8405
0.15	0.8372	0.8361	0.8572	0.8490
0.20	0.8386	0.8378	0.8676	0.8602
0.25	0.8394	0.8395	0.8727	0.8730

5. Conclusions

A comprehensive study into the elastic buckling of outstand SC bimetallic plates subjected to uniaxial compression has been presented. Taking the neutral surface and transverse shear deformation into consideration, the energy method is adopted to derive the analytical solutions of the buckling stress. The FE models are developed in both MATLAB and ABAQUS to verify the accuracy of theoretical solutions, in which different combinations of parameters like clad ratios, width-to-thickness ratios, aspect ratios and cladding materials are used for the purpose of validation. The validated formulae have been used to carry out a series of parametric analyses to further clarify the influence of critical parameters. Finally, in combination of the previous research findings, a comprehensive design method for SC bimetallic plates has been proposed, including a set of formulae to calculate the elastic buckling stress. Detailed findings are outlined as follows:

(1) The energy method with Ritz formulation can be adopted to solve the buckling stress of outstand SC bimetallic steel plates, while the relative position of neutral surface from the middle one z_{n}, the bending stiffness D and the first-order shear deformation effect have been considered to improve the accuracy;

(2) Numerical analyses based on two FE analysis tools (MATLAB and ABAQUS) have been conducted, and the results obtained through these two methods show complete consistency with each other as well as with the theoretical solutions;

(3) The influence of clad ratio on the buckling stress is mainly controlled by the bending stiffness, and the patterns of SP and DP are different;

(4) The influence of width-to-thickness ratio on the buckling stress is more significant compared to that of the clad ratio;

(5) When the aspect ratio is small, the change of the plate shape can lead to a considerable variation of buckling stress;

(6) When the material properties of the cladding and substrate materials are significantly different such as the case of TC bimetallic steel, the slight change of other parameters can cause a big change in the buckling stress;

(7) For internal and outstand bimetallic steel plates, the boundary conditions can significantly affect the buckling stress, but the influence of parameters is similar;

(8) Combining the design formulae of internal and outstand bimetallic stel plates, an integrated design method have been proposed to calculate the elastic buckling stress of bimetallic steel plates.

References

[1] Ban H. Y., Mei Y. X., Shi Y. J., "Research advances of stainless-clad bimetallic structures", Engineering mechanics, 38(6), 1-23, 2021 (in Chinese).
[2] Ban H. Y., Bai R. S. Yang L., Bai Y., "Mechanical properties of stainless-clad bimetallic steel at elevated temperatures", Journal of Constructional Steel Research, 162, 105704, 2019.
[3] Ban H. Y., Bai R. S., Chung K. F., Bai Y., "Post-fire material properties of stainless-clad bimetallic steel", Fire Safety Journal, 112, 102964, 2020.
[4] Ban H. Y., Yang K. H., Mei Y. X., "Experimental study of corrosion resistance of stainless-clad bimetallic steel and welded connections", Journal of Tianjin University (Science and Technology), 54(2), 111–121, 2021 (in Chinese).
[5] Ban H. Y., Zhu J. C., Shi G., Zhang Y., "Tests and modelling on cyclic behaviour of stainless-clad bimetallic steel", Journal of Constructional Steel Research, 166, 105944, 2020.
[6] Mei Y. X., Ban H. Y., "High strain rate behaviour of stainless-clad bimetallic steel", Engineering Structures, 207, 110219, 2020.
[7] Mei Y. X., Ban H. Y., Shi Y. J., "Elastic buckling of simply supported bimetallic steel plates", Journal of Constructional Steel Research, 198, 107581, 2022.
[8] Ban H. Y., Mei Y. X., "Local buckling behaviour of stainless-clad bimetallic steel built-up square hollow section stub columns", Thin-Walled Structures, 182, 110207, 2023.
[9] Ban H. Y., Zhu J. C., Shi G., "Cyclic loading tests on welded connections of stainless-clad bimetallic steel and modelling", Journal of Constructional Steel Research, 171, 106140, 2020
[10] Zhang D. G., Zhou Y. H., "A theoretical analysis of FGM thin plates based on physical neutral surface", Computational Materials Science, 44, 716–720, 2008.
[11] Karamanli A., Aydogdu M., "Bifurcation buckling conditions of FGM plates with different boundaries", Composite Structures, 245, 112325, 2020.
[12] Chen J., Stability of Steel Structures: Theory and Design (6th Edition), Science Press, Beijing, 2011 (in Chinese).
[13] Ferreira A. J. M., Fantuzzi N., MATLAB Codes for Finite Element Analysis, Springer, 2020
[14] Standard for Design of Steel Structures (GB 50017-2017), China Architecture & Building Press, Beijing, 2018 (in Chinese).
[15] Code for Technical specification for stainless steel structures (CECS 410:2015), China Planning Press, Beijing, 2015 (in Chinese).

Acknowledgement

This study was financially supported by the National Natural Science Foundation of China (No. 52078272, 51778329), which is gratefully acknowledged.